Height restriction barriers detection from traffic scenarios using stereo-vision

Maria-Irina Barbu, Ion Giosan, Tiberiu Marița
Computer Science Department
Technical University of Cluj-Napoca, Romania
Irina.M.Barbu@gmail.com, {Ion.Giosan, Tiberiu.Marita}@cs.utcluj.ro

***Abstract*—Height restriction barriers detection is important usually for trucks' driving assistance systems. In this paper we propose a novel approach that uses stereo-vision and combines intensity and depth information for height barriers detection and tracking. High quality stereo-reconstruction is carried out by the SORT-SGM algorithm. Canny edges are extracted from 2D intensity image and filtered out by the 3D information. Horizontal lines are determined using the Hough transformation on the filtered edges and then validated by an intensity correlation approach taking into consideration that usually height restriction barriers have a repetitive textural pattern. Neighboring lines are clustered together in order to form the barrier region of interest. The height of the barrier is also approximated from the 3D points that belong to the barrier's region of interest. SURF features are extracted for the detected barriers from the intensity image and used for tracking them across frames. The whole height restriction barriers detection system performs real time with high accuracy results.**

Keywords—height restriction barriers; intensity information; depth information; detection; height estimation; tracking

I. INTRODUCTION

Nowadays, driving assistance systems are frequently used in many intelligent vehicles. The most common functions integrated in a driving assistance system are: obstacle collision warning, speed keeping assistance, lane departure warning, lane keeping assistance, traffic sign recognition, pedestrian collision warning and avoidance etc. These are used in on-board driving assistance systems on passenger cars which usually don't have very high height.

Figure 1. Coach collision with a traffic height restriction barrier in Tianjin, China [1]

In case of busses and trucks, their higher heights may cause unexpected collisions with traffic height restriction barriers due to the driver inattention or even due to the fact that their height is not signalized and the driver doesn't correctly appreciate it (see Figure 1). This motivates the researchers for developing robust solutions for preventing and avoiding any collisions of busses or trucks with height restriction barriers.

Many different sensors like RADARs, LIDARs, ultrasound sensors, infrared sensors and video cameras may be used for acquiring the traffic scene information. Among these sensors, we prefer a pair of two gray levels cameras in stereo setup for scene images acquisition. Stereo-vision [2] offers both pixel intensity information and also the possibility of computing depth. Usually the obstacles' texture [3] may be detected from the intensity images while the depth information [4] may be very useful for search space reduction and for validating them [5]. In our case, we are focusing on detecting the height restriction barriers' regions of interests in the traffic scenes by using both intensity and depth information. A barriers detection method using stereovision was proposed in [6], but the subject is not so common in the literature.

A high quality of stereo-reconstruction is absolutely necessary for obtaining high accurate 3D reconstructed scene points. We use the SORT-SGM stereo-reconstruction algorithm [7] implemented on a GPU that offers 3D points accuracy in a very low processing time. Even with a high quality stereo-reconstruction available, the 3D points from the neighborhood of the height restriction barriers are not so accurate or the reconstructed points might be missing. This is due of the fact that stereo cameras are displaced left-right in the stereo setup configuration and the barriers are also horizontal structures.

The methods that perform traffic obstacle detection by means of 3D points grouping [5, 8] cannot be applied for detecting a height barrier. Usually the points that are higher than a specified threshold or they are belonging to hanging obstacles are usually rejected by these approaches because they affect the on-road obstacle detection. Although there are some methods for determining the elevation map [9], road surface [10] or the driving area [11], in our approach we use only the primary 2D intensity information and the 3D reconstructed points and make the assumption of a planar road in front of the ego-vehicle.

We combine the intensity Canny edge detection [12] result with the power of the Hough transform [13] for detecting the barrier's candidate horizontal lines. The assumption of repetitive texture pattern of the height barriers is made and a correlation score computation approach is proposed for selecting the lines that are on the barrier surface. A clustering procedure is also proposed for grouping the barrier's lines with the closest candidate lines in order to determine the entire region of interest of the barrier. A tracking procedure based on SURF features [14] is used for keeping the detected barrier across frames, in the situations when the barrier it is not detected in the current frame but it was previously detected in other frames. All these steps are described in details in the next sections.

II. SYSTEM ARCHITECTURE

In Figure 2, the components of our proposed height restriction barriers detection and tracking system, the relationships between them and also the input and output of each module are depicted.

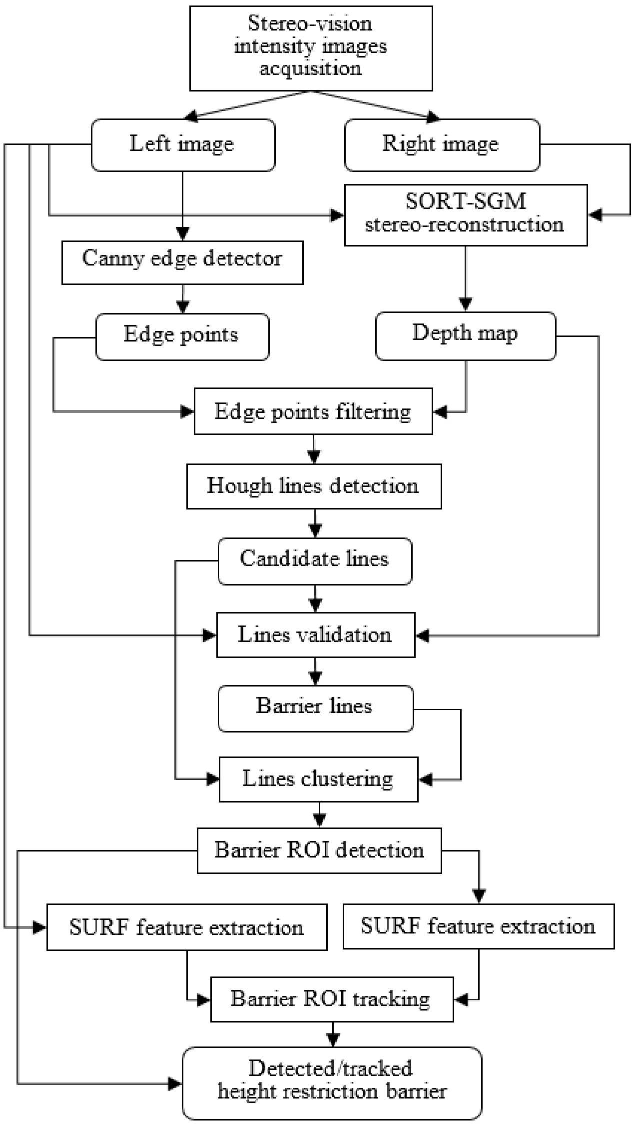

Figure 2. Height restriction barriers detection and tracking system architecture

Gray levels images of the traffic scenes are acquired with a pair of stereo-vision cameras. A high quality stereo-reconstruction is achieved by using the SORT-SGM algorithm [7] which offers accurate and dense depth map, which are very important for the subsequent processing steps. Height restriction barriers are clearly distinguishable from the neighboring background.

Canny algorithm is employed for detecting all the scene edges including those that separates the barriers from the background. In order to select only the edges near the barrier's structure, we filter out all the other edges based on some height constraints. The heights' values are known for all the 3D reconstructed points.

Hough lines detection follows the edge detection. It helps finding the candidate lines of the barrier. Usually the height restriction barriers have a repetitive textural pattern, so a texture correlation validation procedure is proposed for selecting the lines that lie onto the barrier.

Near the true lines of the barrier there may appear some candidate lines that also belong to the barrier, so we cluster all the line candidates with the barrier's lines based on their vicinity. A cluster of lines is considered to define a detected barrier.

Across sequences of multiple frames, there can be few intercalated frames in which the barrier is not detected. This fact can appear due to multiple factors. A tracking procedure based on SURF features of the detected barrier in the previous frames is proposed for solving this problem in the current frame. The output of the entire system consists in signalizing the presence of the height barriers and their corresponding heights in traffic images.

III. METHOD DESCRIPTION

In this section, we describe in details all the modules of the height restriction barriers detection and tracking system.

Stereo-vision grayscale images with 512x383 pixels are acquired. Preprocessing algorithms for correcting the distortions and image rectification are also applied. Stereo-reconstruction is performed using a high quality SORT-SGM algorithm. In Figure 3 we present an example of stereo-reconstructed points. At each row *i* and column *j* in the left image, the corresponding stereo-reconstructed point it is drawn with one of the three different colors cyan, magenta and brown according to its height *Y* in the scene:

$$\text{Color}(Point_{ij}) = \begin{cases} brown, \text{ if } Y(Point_{ij}) > 3000\,\text{mm} \\ cyan, \text{ if } 200\,\text{mm} \le Y(Point_{ij}) \le 3000\,\text{mm} \\ magenta, \text{ if } Y(Point_{ij}) < 200\,\text{mm} \end{cases} \quad (1)$$

The origin (0, 0, 0) of the scene system coordinates (*X*, *Y*, *Z*) is situated exactly in front of the ego-vehicle, in its middle and on the road surface.

a)

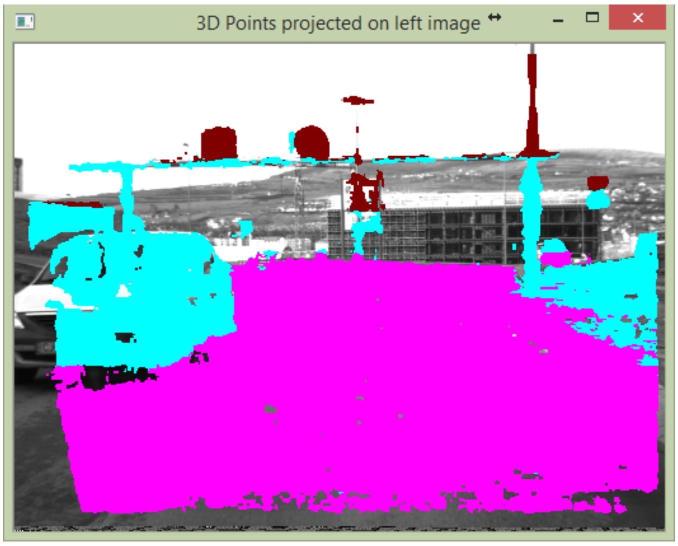

b)

Figure 3. Stereo-reconstruction: a) left intensity image; b) 3D reconstructed points projected onto the left image

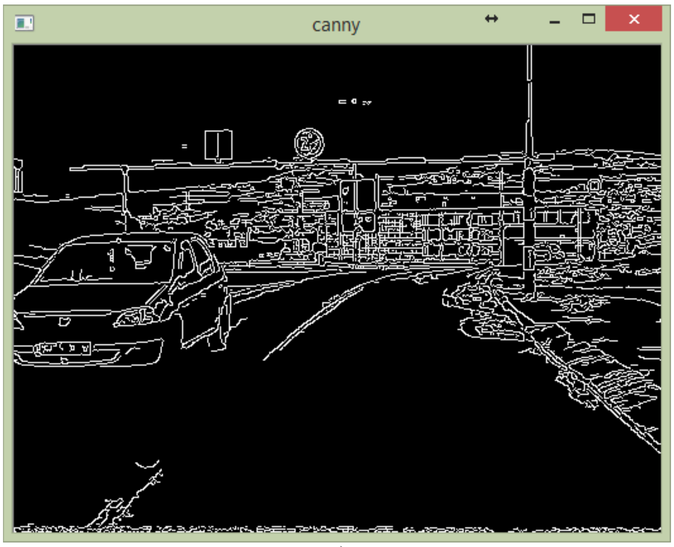

a)

b)

Figure 4. Edges on the left image: a) original edges obtained from the Canny algorithm; b) filtered edges using some constraints

Canny edges are extracted in the left image considering the two hysteresis thresholds T_{low}=50 and T_{high}=200. For the next steps we keep into analysis only the edge points at positions (i, j) that have a stereo-reconstructed point associated which also satisfy the following constraints:

$$\begin{aligned} &Y(Point_{ij}) > 2500\,\text{mm} \\ &Y(Point_{ij}) < 5000\,\text{mm} \\ &Z(Point_{ij}) < 30000\,\text{mm} \end{aligned} \tag{2}$$

The constraints (2) take the assumption that a traffic height restriction barrier is usually placed between 2,5m and 5m height and also restrict the scene searching space not far away than 30m. The extracted edges on the scene depicted in Figure 3 and also the filtered edges that will be used for the next processing steps are presented in Figure 4.

We use a probabilistic Hough method [15] applied on the filtered edges in order to determine all the image lines including the real ones that belong to the height restriction barriers. The parameters determined empirically and set for this method are:

$$\begin{aligned} &d\rho = 1\,\text{pixel} \\ &d\theta = 1^{\circ} \\ &MinVotes = 50 \\ &MinLineLength = 20\,\text{pixels} \\ &MaxLineGap = 40\,\text{pixels} \end{aligned} \tag{3}$$

The lines that are considered to be candidates for the height restriction barrier have a maximum drift of ±5º from the horizontal direction. We make the assumptions of traffic scene scenario with planar roads and the ego-vehicle that is approaching a height barrier having a very small roll angle. Only these lines are considered for the next steps.

Not all these candidate lines are situated on a height restriction barrier. In order to validate them, we analyze the pixel intensities along them with the purpose of selecting only the lines that have the intensities forming a repetitive pattern. We iterate all the pixels located on each candidate line and store them in an array *I*. Several correlation coefficients $Corr_k$ for each intensity lag *k* are computed:

$$\begin{aligned} Corr_k &= \frac{\sum_{\substack{t\in I \\ t+k\in I}} \left|I(t)-I(t+k)\right|}{\|I\|-k}, \\ minCorr &= \min\left(Corr_k\right) \\ maxCorr &= \max\left(Corr_k\right) \\ k &\in \left[lowLag,\ highLag\right] \end{aligned} \tag{4}$$

The drift range for *k* was selected empirically: *lowLag*=10, *highLag*=70. The minimum and maximum values for all the correlation coefficients are computed and the line is considered to be part of a height restriction barrier only if these two boundary values are satisfying the following conditions:

$$\begin{aligned} minCorr &< lowThresholdCorr \\ maxCorr &> highThresholdCorr \end{aligned} \tag{5}$$

We use the two thresholds values: *lowThresholdCorr*=50 and *highThresholdCorr*=85. It is obvious that there can exist other candidate lines that are close to these height restriction barrier detected lines and which should be taken into consideration. A clustering procedure is proposed in order not to miss detect some candidate lines. Every barrier detected line *d* form a cluster with other candidate line *c* if the extremities of the candidate line P_{1c} and P_{2c} are closer than a threshold *tBetween*=10 to the detected line and there is at least one point P_{1c} or P_{2c} closer than a threshold *tAway*=40 from one of the extremities P_{1d} or P_{2d} of the detected line:

$$\begin{aligned} & d(P_{1d}, P_{2d}),\ c(P_{1c}, P_{2c}) \\ & distance(d, P_{1c}) < tBetween \\ & distance(d, P_{2c}) < tBetween \\ & \exists (i,j) \mid P_i \in \{P_{1c}, P_{2c}\} \wedge P_j \in \{P_{1d}, P_{2d}\} \wedge \\ & \qquad distance(P_i, P_j) < tAway \end{aligned} \tag{6}$$

After this step, a number *nc* of barrier lines clusters C_i, each containing one pure detected barrier line and other candidates are formed. The bounding rectangle $boundingRectangle_i$ of every cluster is determined and the real height restriction barrier bounding rectangle *barrierRectangle* is chosen to be the widest one:

$$barrierRectangle = \underset{\substack{i\in C_i \\ i=1,nc}}{widest}(boundingRectangle_i) \tag{7}$$

In Figure 5, the bounding rectangle of the height restriction barrier is drawn with blue color. It is the largest cluster from all the clusters containing the detected barrier lines and the candidate lines that were validated with the constraints (6).

Figure 5. Height restriction barrier bounding rectangle (with blue color); detected barrier lines (red color); valid candidate lines (green color)

For approximating the barrier's height we take into consideration all the reconstructed 3D points closer than 30m which have the 2D left image projections inside the previously determined bounding barrier rectangle. The height of the barrier is selected to be the median value of the heights:

$$\begin{aligned} Heights = \{ & Y(Point_{ij}) \mid Z(Point_{ij}) < 30000\,\mathrm{mm} \wedge \\ & Projection(Point_{ij}) = P_{ij} \wedge \\ & P_{ij} \in barrierRectangle \} \\ barrierHeight &= median(Heights) \end{aligned} \tag{8}$$

Figure 6. Detected height restriction barrier (bounding rectangle with red color) with the specified height above (with blue color)

The computed height (with approximation of one decimal) for the detected height restriction barrier in the current frame is displayed above its bounding rectangle (see Figure 6).

According to our methods steps proposed above for height restriction barrier detection, there can appear few intercalated frames in a sequences of frames in which the proposed methodology doesn't detect any barrier even if it is present. In order to fill in these gaps we propose a tracking procedure of the detected barriers in consecutive frames. This will increase the robustness of our method.

The SURF key points *K* and the associated feature vector *FV* to every key point are extracted from the detected barrier bounding rectangle in the frame *P*. The tracking procedure is applied in the case when in the current frame *C* there isn't detected any barrier and in the previous frame *P* existed one. The same key points and feature vectors are extracted for the scene in the current frame. A fast approximated nearest neighbor search algorithm [16] is used for matching the barrier's features from the previous frame against the scene features. The barrier is considered to be tracked only if the minimum matching score distance is lower than a threshold *tFeatDist*=0.02:

$$\begin{gathered} K = \{k_i\},\ FV = \{FV_i\},\ i = 1, \ldots, nrKeyPoints \\ \min_{i=1,\|K\|}\left(distance(FV_P, FV_C) \right) < tFeatDist \end{gathered} \quad (9)$$

We find then a perspective transformation between the previous frame *P* and the current frame *C* by applying a RANSAC algorithm [17] on the matching pairs of key points between the detected barrier in frame *P* and the corresponding points in the current frame *C*. The RANSAC algorithm finds the perspective transformation matrix parameters *M*. The bounding rectangle of the barrier in the previous frame *P* is projected into the current frame *C* by using the transformation matrix *M*.

A final refinement is employed for filtering out spurious tracked barriers. The number of edge filtered points that are inside the barrier bounding rectangle in the current frame *C* are counted. It is used for computing the edges density in the barrier bounding rectangle. A barrier is considered to be a good track only if it has the edge points' density above a threshold *tEdges*=0.1:

$$\begin{gathered} EP = \{Point_{ij} \mid (i,j) \in boundingRectangle\} \\ edgeDensity = \frac{\|EP\|}{Area(boundingRectangle)} \\ edgeDensity > tEdges \end{gathered} \quad (10)$$

In Figure 7, an example of a tracked height restriction barrier is presented. The image represents the next frame of the image from Figure 6, where a detected height restriction barrier was detected. The bounding rectangle in Figure 7 is obtained by the perspective projection of the previous frame barrier bounding rectangle and it is drawn with the magenta color. The height of the tracked barrier is displayed above and it is copied from the previously detected barrier.

Figure 7. Tracked height restriction barrier (bounding rectangle with magenta color) of the detected barrier from Figure 6

IV. Experimental Results

In this section, we present the proposed height restriction barrier detection and tracking system's results. The results were obtained from two stereo-vision image sequences containing height restriction barriers having thousands of frames.

In terms of qualitative evaluation shows that the height restriction barriers in front of the ego vehicle are well detected and tracked. Miss detections can occur due to some poor stereo-reconstructed points around the barrier or due to the dirt on the barrier's surface that sometimes may affect the correlation score of checking the repetitive textural pattern. False alarms may occur in scenarios with non-planar road surface where the estimated heights aren't correct at all or rarely on frontal buildings with many horizontal edges and repetitive texture.

Some sample results including three correctly detected barriers and a false positive are presented in Figure 8.

a)

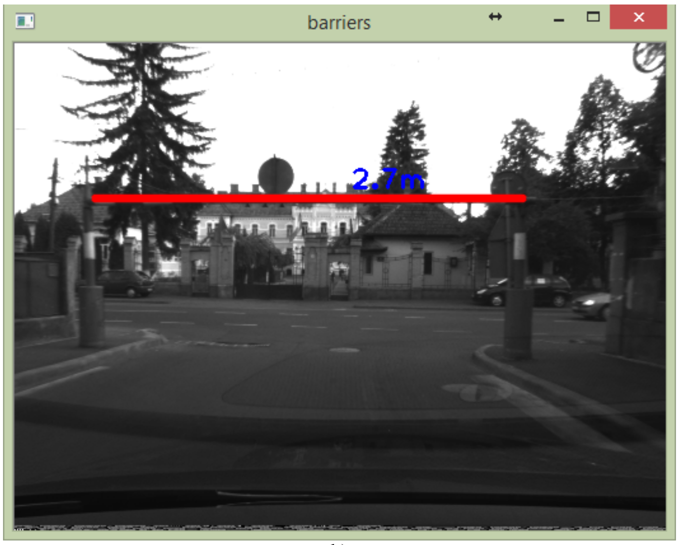

b)

c)

d)

Figure 8. Sample results of height restriction barriers detection: a)-c) true positives; d) false positive

In terms of quantitative evaluation, the system has the following performance:

- approx. 95% true positive rate in height barriers' detection
- less than one false positive height barrier detected at 200 frames
- barriers' height estimation error in the range of [–0.2m, +0.2m]

All the experiments were done in good weather conditions with high visibility traffic environment. Adverse conditions like rain, night time, fog are obviously reducing the system's performance. However these scenarios were not investigated and they are beyond the scope of this paper.

The entire processing necessary for the height restriction barriers' detection and tracking was done on a single core of an Intel Core i7-4790 processor @ 3.60 GHz, the system achieving an execution time less than 40ms/frame, resulting a processing power of more than 25 fps.

V. Conclusions

We proposed a novel approach for height restriction barriers' detection and tracking by processing stereo-vision images. Our method can be successfully integrated within an advanced driving assistance system for avoiding impacts with these kind of structures.

The system combines the 3D information used for reducing the search space with the 2D intensity information that offers the possibility of horizontal structures' detection and their validation by analyzing the repetitive textural patterns specific to height restriction barriers. These structures are clustered together in order to determine the bounding rectangle of the height restriction barriers.

A tracking procedure is also proposed for improving the previously mentioned detection method in order to achieve continuous detections in consecutive frames. The system performs real time and offers high accuracy results.

As a future work, in order to improve the system's performance, we investigate the possibility of using a road surface estimation module which eliminates the flat road assumption and a better module for validating the barriers' lines by considering multiple features not only on their repetitive textural pattern. It would be also great to investigate the possibility of detecting the height restriction barriers in low-visibility traffic scenarios in order to help the driver avoiding such an obstacle in difficult visibility conditions.

Acknowledgment

This work has been supported by UEFISCDI (Romanian National Research Agency) in the national research project Multi-scale Multi-modal Perception of Dynamic 3D Environments Based on the Fusion of Dense Stereo, Dense Optical Flow and Visual Odometry Information (MultiSens), project code PN-II-ID-PCE-2011-3-1086.

References

[1] ChinaDaily.com.cn. (2015). *At least 2 dead, dozens hurt after bus hits road barrier*. Available: http://www.chinadaily.com.cn/china/2015-01/26/content_19410897.htm

[2] S. Nedevschi, R. Danescu, D. Frentiu, T. Marita, F. Oniga, C. Pocol*, et al.*, "High accuracy stereo vision system for far distance obstacle detection," in *IEEE Intelligent Vehicles Symposium*, 2004, pp. 292-297.

[3] J. Malik, S. Belongie, T. Leung, and J. Shi, "Contour and Texture Analysis for Image Segmentation," *International Journal of Computer Vision,* vol. 43, pp. 7-27, 2001.

[4] Z. Zhen, W. Yifei, J. Brand, and N. Dahnoun, "Real-time obstacle detection based on stereo vision for automotive applications," in *European DSP Education and Research Conference*, 2012, pp. 281-285.

[5] C. Pocol, S. Nedevschi, and M. M. Meinecke, "Obstacle Detection Based on Dense Stereovision for Urban ACC Systems," in *International Workshop on Intelligent Transportation (WIT)*, Hamburg, Germany, 2008, pp. 13-18.

[6] T. Marita, "Barriers detection method for stereovision-based ACC systems," in *Proceedings of International Conference on Intelligent Computer Communication and Processing* 2009, pp. 95-101.

[7] C. D. Pantilie and S. Nedevschi, "SORT-SGM: Subpixel Optimized Real-Time Semiglobal Matching for Intelligent Vehicles," *IEEE Transactions on Vehicular Technology,* vol. 61, pp. 1032-1042, 2012.

[8] C. Pocol, S. Nedevschi, and M. A. Obojski, "Obstacle Detection for Mobile Robots, Using Dense Stereo Reconstruction," in *IEEE International Conference on Intelligent Computer Communication and Processing*, 2007, pp. 127-132.

[9] F. Oniga, S. Nedevschi, M. M. Meinecke, and T. Thanh-Binh, "Road Surface and Obstacle Detection Based on Elevation Maps from Dense Stereo," in *IEEE Intelligent Transportation Systems Conference*, 2007, pp. 859-865.

[10] F. Oniga and S. Nedevschi, "Processing Dense Stereo Data Using Elevation Maps: Road Surface, Traffic Isle, and Obstacle Detection," *IEEE Transactions on Vehicular Technology,* vol. 59, pp. 1172-1182, 2010.

[11] R. Danescu, F. Oniga, and S. Nedevschi, "Modeling and Tracking the Driving Environment With a Particle-Based Occupancy Grid," *IEEE Transactions on Intelligent Transportatin Systems,* vol. 12, pp. 1331-1342, 2011.

[12] J. Canny, "A Computational Approach to Edge Detection," *IEEE Transactions on Pattern Analysis and Machine Intelligence,* vol. 8, pp. 679-698, 1986.

[13] R. O. Duda and P. E. Hart, "Use of the Hough transformation to detect lines and curves in pictures," *Communications of the ACM,* vol. 15, pp. 11-15, 1972.

[14] H. Bay, A. Ess, T. Tuytelaars, and L. V. Gool, "Speeded-Up Robust Features (SURF)," *Journal of Computer Vision and Image Understanding,* vol. 110, pp. 346-359, 2008.

[15] J. Matas, C. Galambos, and J. Kittler, "Robust Detection of Lines Using the Progressive Probabilistic Hough Transform," *Computer Vision and Image Understanding,* vol. 78, pp. 119-137, 4// 2000.

[16] M. Muja and D. G. Lowe, "Fast approximate nearest neighbors with automatic algorithm configuration," in *VISAPP International Conference on Computer Vision Theory and Applications*, 2009, pp. 331-340.

[17] M. A. Fischler and R. C. Bolles, "Random sample consensus: a paradigm for model fitting with applications to image analysis and automated cartography," *Communications of the ACM,* vol. 24, pp. 381-395, 1981.